



Preprocess-Optimization for Polypropylene Laser Sintered Parts

Thomas Reinhardt¹, Alexander Martha², Gerd Witt³ and Peter Köhler⁴

¹University of Duisburg-Essen, thomas.reinhardt@uni-due.de

²University of Duisburg-Essen, alexander.martha@uni-due.de

³University of Duisburg-Essen, gerd.witt@uni-due.de

⁴University of Duisburg-Essen, peter.koehler@uni-due.de

ABSTRACT

Additive manufacturing delivers the opportunity to manufacture complex geometry with comparable effective effort. Nevertheless, comprehensive information for the sufficient configuration of the process and related parameters are still missing. Here joint researches of the chairs for Manufacturing Technology and Computer Aided Design at the University of Duisburg-Essen were carried out in order to receive detailed information about the influencing factors on part quality for polypropylene laser sintering parts. These experimental results provided the basis for the development of software supported applications for the preprocess optimization.

Keywords: rapid prototyping, additive manufacturing, laser-sintering, part orientation, build direction.

DOI: 10.3722/cadaps.2013.xxx-yyy

1. INTRODUCTION

Additive Manufacturing (AM) refers to a group of technologies used for producing prototypes (Rapid Prototyping), tools and molds (Rapid Tooling) and end products (Rapid Manufacturing). Due to the additive process which builds up the physical part layer by layer, geometries of any complexity like undercuts and internal features can be built, because the whole geometry of the part is not of importance in the current layer. So during the last years AM is successfully used as an effective tool for the rapid development of products of nearly any complexity [7,14].

Every AM process is characterized by the preprocessing, the build process and the postprocessing [12]. Common for all layered manufacturing techniques is that part-quality and manufacturing costs depend on the part orientation during the process. The result is that different parameters must be balanced in order to find a good orientation for each part. Based on the "optimal" orientation, the different parts are positioned inside the build chamber of the AM machine. Hence, the orientation of parts is influenced by several different parameters, difficulties occur when the best orientation has to be found. State of the art software does not deliver adequate solutions for this problem. Therefore, the user

has to identify good part orientations based on his experience. Here a number of orientation-dependent effects such as stair-stepping, anisotropic material properties like mechanical strength and shrinkages must be considered for the correct choice of part orientation. Usually this circumstance can be reduced by selecting suitable process parameters (laser beam power, scan speed) and building strategies (scan strategy, shrinkage compensation). Additionally the consideration of the AM process within an economic point of view becomes increasingly important. Beside the fixed costs, such as capital, labor and maintenance costs, the variable costs (material and operating costs) are significantly responsible for the total costs. For that reason the selection of the part orientation must be considered as part of the total construction costs, which are reflected by the building time, the wasted powder and necessary preparation and finishing steps.

All in all, the procedure of the correct orientation becomes more and more difficult with increasing part complexity and necessitates a software-aided support for the user in order to generate an effective solution. Here, research activities were carried out in order to find an optimal part orientation with software support. For the available approaches, most of

the influencing factors are only considered comprehensive and the geometry is usually limited to simple or convex parts. [4,5]. In this regard PHAM et al. [10], YANG et al. [15], MAASOD and RATTANAWONG [9] and XU et al. [16] created solutions for one single or just a little influence factors. CHENG et al. developed an approach for the classification of surfaces in association with part accuracy [3]. In order to create a solution with an effective solution finding different approaches with used evolutionary algorithms for the task of multi-objective optimization were developed by e. g. BYUN and LEE [2] and TYAGI et al. [13]. These considerations were taken into account for the developments of DANJOU and KÖHLER at the University of Duisburg-Essen [4-6]. This multi-objective approach is used for the presented examples in this paper. Beyond that some adjustments based on the realized experiments have been applied.

These adjustments are mostly necessary because the prior developments were developed based on the part hence reliable information for special AM technologies were inadequate. Therefore this paper describes methods how this necessary information can be gained by experiments and then be transferred to a software based orientation optimization. The described research was carried out for laser-sintering. Laser-sintering is an AM technology that uses a laser in order to fuse plastic powder. Based on 3D-CAD data the original geometry is sliced in order to manufacture a layer by layer generated 3D model. In this case polypropylene is used as process material.

2. EXPERIMENTAL SETUP

Preliminary findings show, that the powder bed temperature, the power of outline and fill laser, the scan speed, the fill scan spacing as well as the layer thickness are significant parameters for laser-sintered part properties [1,8,11]. Here the mechanical properties rise as a function of the energy density of the laser. Simultaneously the geometric specifications, such as the surface roughness or the dimensional accuracy get worse with a high energy density. Illustrated researches examine just the influence of process parameters and orientation to single quality values.

Research, related within this paper carries the studies forward by a simultaneous optimization of the process parameters for different target values. The development of multi-objective optimization strategies are supposed to ensure a part orientation, which considers manufacturing and functional aspects based on previous findings [4,5].

In the course of investigations 2 test body geometries were designed to fulfill the different measuring tasks. With the test body geometry shown in figure 1 a) the accuracy of parts generated by laser sintering of laser-sintered parts can be evaluated. First the surface roughness as a function of the surface's orientation will be analyzed. Therefore the test body geometry consists of 13 different surface orientations, in detail six upward facing surfaces ($0^\circ, 15^\circ, 30^\circ, 45^\circ, 60^\circ, 75^\circ$) and seven downward facing surfaces ($0^\circ, 15^\circ, 30^\circ, 45^\circ, 60^\circ, 75^\circ, 90^\circ$) with each length of 25 mm were considered. To measure the surface roughness, a Mitutoyo tactile surface measurement system SJ-400 was used. According to DIN EN ISO 4288, both the arithmetical means roughness R_a and the surface roughness depth R_z were examined. Second the dimensional accuracy can be measured by taking the dimensions in any direction ($x = 37,5 \text{ mm}$, $y = 30 \text{ mm}$ and $z = 26 \text{ mm}$). To characterize the shape stability, different form elements were determined, marked with green notes in figure 1a. To accomplish the complete dimensional analysis, the 3D Scanning System ATOS III Triple Scan by the Company GOM was used to capture all test body geometries full surfaces geometry with a precisely dense cloud mesh.

Another source of inaccuracy is curl, which results in curved edges of the part. Therefore a second test body geometry was designed, as shown in figure 1b. The maximum length of the part is limited to $x = 140 \text{ mm}$ and the width is limited to $y = 10 \text{ mm}$. The part thickness is kept to $z = 10 \text{ mm}$. The main objective is to measure the degree of curl along the bottom length of the part. To measure the curl effect, a coordinate measuring machine C3 5-4-4 from Nikon was used. The upward facing surface was scanned with a tactile sensor for the whole length. Additionally both the starting and ending measuring point were captured three times for statistical reasons.

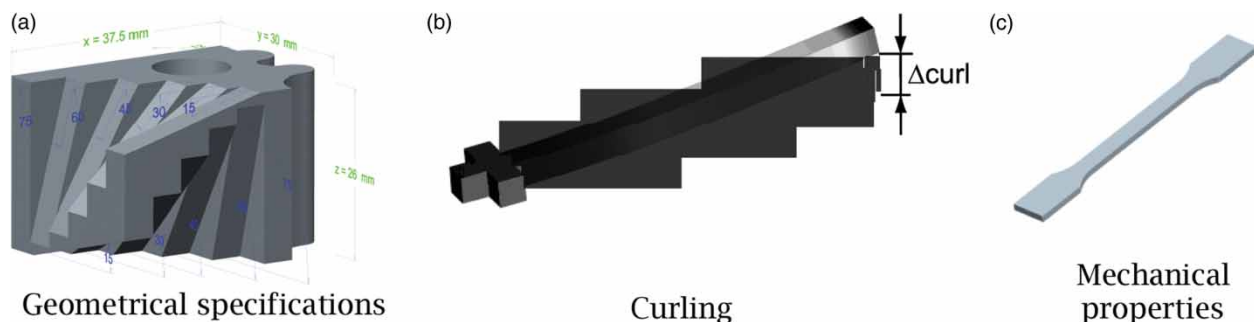


Fig. 1: Investigation of the main quality characteristics with defined test geometries.

Nr	Process parameters	Unit	Levels	1	2	3	4
A	Powder bed temperature	[°C]	4	139	140	141	142
B	Extraction chamber temperature	[°C]	4	100	110	120	130
C	Fill laser power	[W]	4	8	10	12	14
D	Layer thickness	[mm]	4	0,08	0,10	0,12	0,14
E	Outline scan speed	[mm/s]	4	2500	2700	2900	3100
F	Outline laser power	[W]	4	6	8	10	12
G	Hatch spacing	[mm]	4	0,22	0,24	0,26	0,28
H	Fill scan speed	[mm/s]	4	2800	3000	3200	3400
I	Distance Outline - Fill	[mm]	4	0,03	0,09	0,15	0,21

Tab. 1: Chosen influencing factors and parameter levels.

Initially the main influencing factors of the laser-sintering process for defined quality characteristics have to be identified. Therefore nine different parameters which are varied in four different levels were chosen for the analyses. From the current author experience, those parameters which exert a direct influence on the energy input of the powder both of outline and fill exposure, apparently have a major impact on the process quality. The Energy density can be expressed as shown in Equation (1).

$$E = \frac{P_L}{v_L \times h_s \times l} \quad (1)$$

Here, E is the energy density [J/mm³], l is the layer thickness [mm], P is the laser power [W], v_L the beam speed [mm/s] and h_s the hatch spacing [mm]. Preliminary test showed that the processing of polypropylene can be handled with an volume energy density within the limits $E_{\min} = 0,09$ J/mm³, and $E_{\max} = 0,22$ J/mm³. Therefore, the range of the laser power, laser beam scan speed and hatch spacing of the fill exposure were selected as 8 to 14 W, 2800 to 3400 mm/s and 0,22 to 0,28 mm. The range of the outline exposure parameters like laser power and laser beam scan speed was set to 6 to 8 W and 2500 to 3100 mm/s. Furthermore both the layer thickness and the space between outline and fill exposure were investigated. Additionally process temperatures such as the powder bed temperature (139 to 142°) and extraction chamber temperature (100 to 130°) were considered. All process variables and their levels are summarized in table 1.

To perform the analyses, the robust design method of Taguchi is used. Here not all possible combinations of the chosen process parameters, but a selected subset were performed, without reducing the information value of the analyses [4]. In this case, the array L'32 was chosen. To analyze the results, two different evaluation methods were used. First the signal-to-noise (S/N) is used to compare a collection of means, rates or proportions. The optimal settings for each parameter are given, when the S/N ratio assumes an extreme. Depending on the demand either the minimization problem, as shown in Equation (2), or the maximization problem, as shown in Equation (3),

is used. Within an ANOM decision chart the group means are plotted to determine the significance of the control parameters. Second the analysis of variance (ANOVA) is used to identify and analyze significant or pooled factors.

$$\eta = -10 \log_{10} \left(\frac{1}{n} \sum_{i=1}^n y_i^2 \right) \quad (2)$$

$$\eta = -10 \log_{10} \left(n \sum_{i=1}^n y_i^2 \right) \quad (3)$$

In the course of investigations the minimization problem is used to identify the main influences of the process parameters on the geometrical properties like surface roughness, dimensional accuracy and shape stability. The maximization problem is used for detecting best mechanical properties.

The studies were performed on an EOS Formiga P100 laser-sintering machine. The material that was investigated in this paper is a polypropylene with 20% glass beads. In total 16 jobs were built, including all necessary 32 experiments, as shown in figure 2a. To expose the influence of the part orientation, the test body geometries were built in the directions 0°, 15°, 30°, 45°, 60°, 75° and 90° related to the building platform, see figure 2b.

3. RESULTS AND DISCUSSION

3.1. Process Optimization

As a result of this chapter the laser-sintering process shall be optimized under the consideration of the relationship between the process parameter, the part orientation and the part properties.

3.1.1. Dimensional accuracy and shape stability

All 32 test body geometries were captured with a dense cloud mesh. For the evaluation of the dimensional accuracy, the deviations in every dimension were measured. To examine shape stability the diameter of the hole and concave and convex surfaces were analyzed. Using the problem of minimization (Equation 2) the factor effects were examined. The

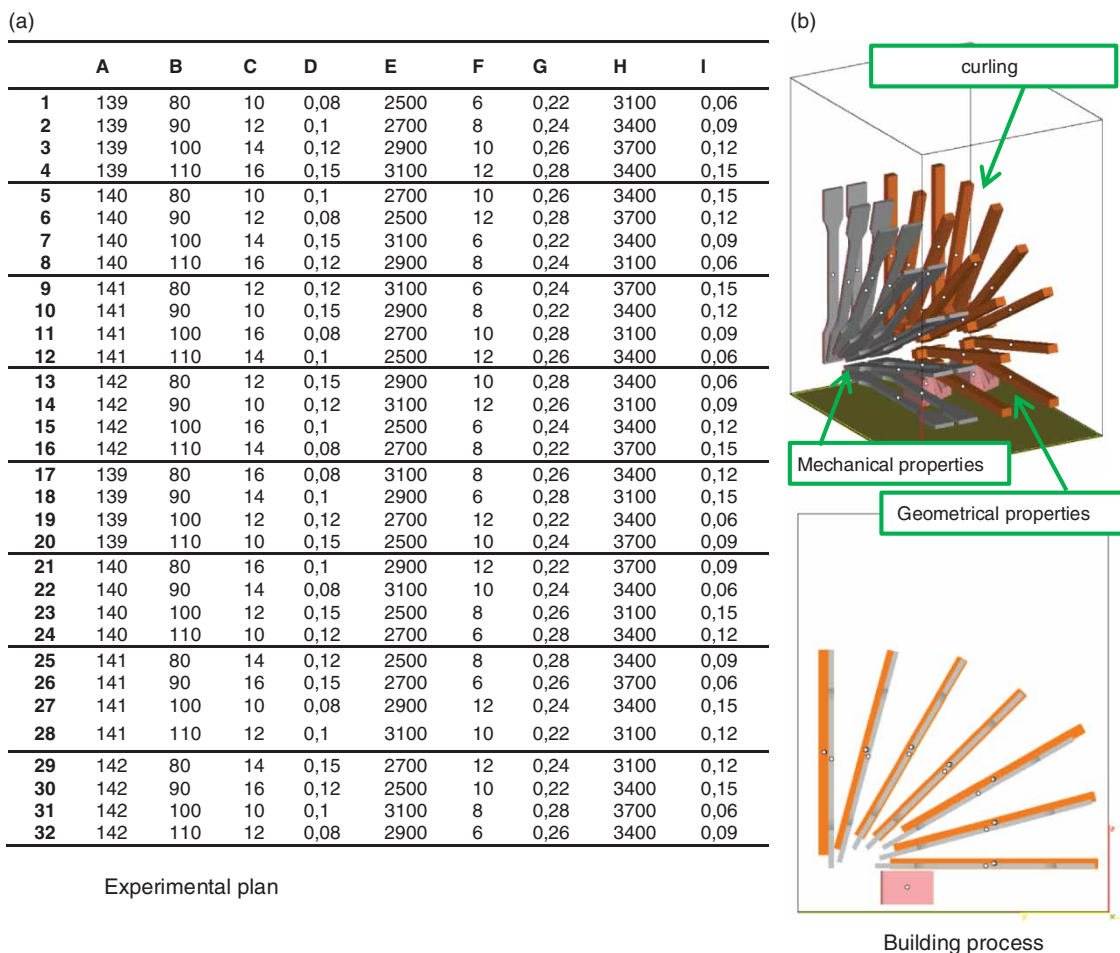


Fig. 2: Test execution.

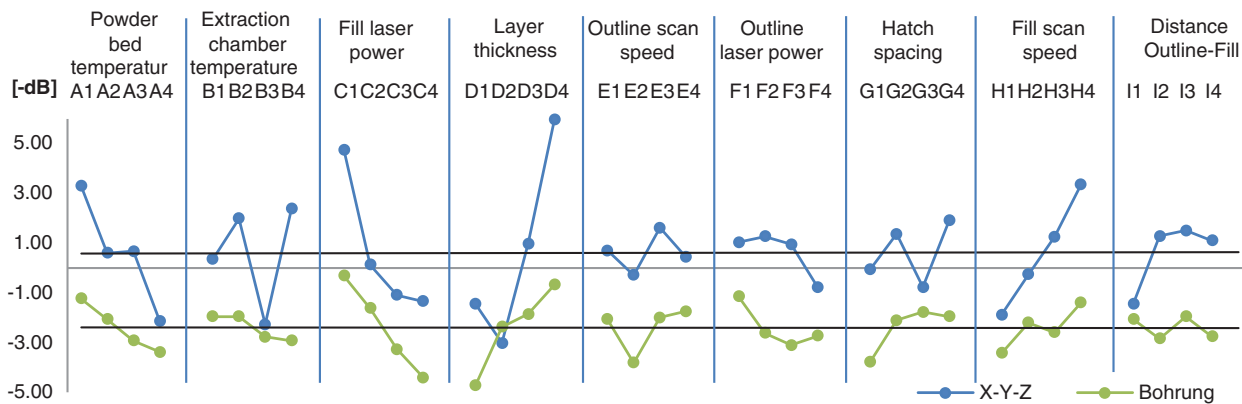


Fig. 3: ANOM chart for dimensional accuracy and shape stability.

effects of all considered factors to the dimensional accuracy and the shape stability are shown in figure 3.

First the S/N Ratio for both investigated targets are very similar. The largest span has the layer thickness and is therefore the most important factor. Contrary to the expected adoption, the geometrical specifications are reduced with a decreasing layer

thickness. Reasons can be found in the energy introduced to the power. The more energy is used to melt down the powder, the more powder adhesion on the surface of the part can be observed. For demonstration reasons a test body geometry build with a high energy density is shown in figure 4.

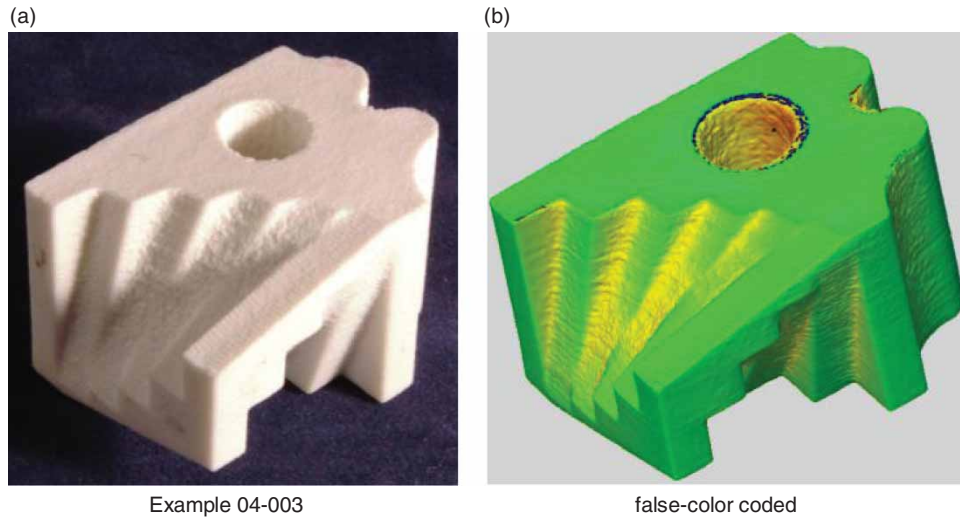


Fig. 4: Effects of high energy density.

Faktor	Dimensional accuracy		Shape stability	
	Sig	p[%]	Sig	p [%]
A Powder bed temperature	*	8,21		5,75
B Extraction chamber temperature	*	7,20		0,04
C Fill laser power	**	15,19	**	26,84
D Layer thickness	**	31,63	**	23,50
E Outline scan speed	X	-		5,68
F Outline laser power	X	-		4,34
G Hatch spacing		0,65		5,27
H Fill scan speed	*	8,27		3,95
I Distance Outline - Fill	X	-	X	-

Tab. 2: ANOVA table for dimensional accuracy and shape stability.

The trend both of the fill laser power and the fill scan speed validate the assumption, that the supplied energy density has a major influence on the geometrical specifications. The results were examined with the ANOVA analyses, as shown in table 2. Here the significance of the process parameters is shown. All parameters with a blue field are pooled, that means their effect on the target is negligible. Light green fields point out a significant factor, dark green fields a highly significant factor. All in all ANOVA confirms the ANOM Analysis. The powder layer thickness has the highest influence with 32% respectively 24%. Furthermore the laser power of the fill exposure is highly significantly important for geometrical specifications. A third main influencing factor is the temperatures of both the powder bed and extraction chamber. Increasing processing temperatures lower the dimensional accuracy and shape stability. The effects of the outline density (outline scan speed and laser power) and the distance from outline to fill exposure are negative and therefore allocated to the share of defects.

3.1.2. Surface Roughness

A total of 416 surfaces were measured. A detailed presentation of the investigations made would exceed the scope of this paper. Therefore the ANOM analysis of the 30° downward facing surface is shown in figure 5 representatively. First of all, the findings show nearly equal results for both targets (R_a and R_z). For every factor concordant optimal parameter settings are proposed. Again the powder layer thickness has the highest influence on the surface roughness. The reason for the high influence can be found in the effect of stair stepping. A low powder layer thickness decreases the effect. Second the laser power and scan speed of the fill exposure have a main influence on surface roughness. Assessing the energy density of the outline exposure, the surface finish improves with increasing energy density, but after a certain value the surface quality deteriorates.

Table 3 summarizes the number of significant, random influences and pooled factors in dependence of the orientation. Regardless to the surface

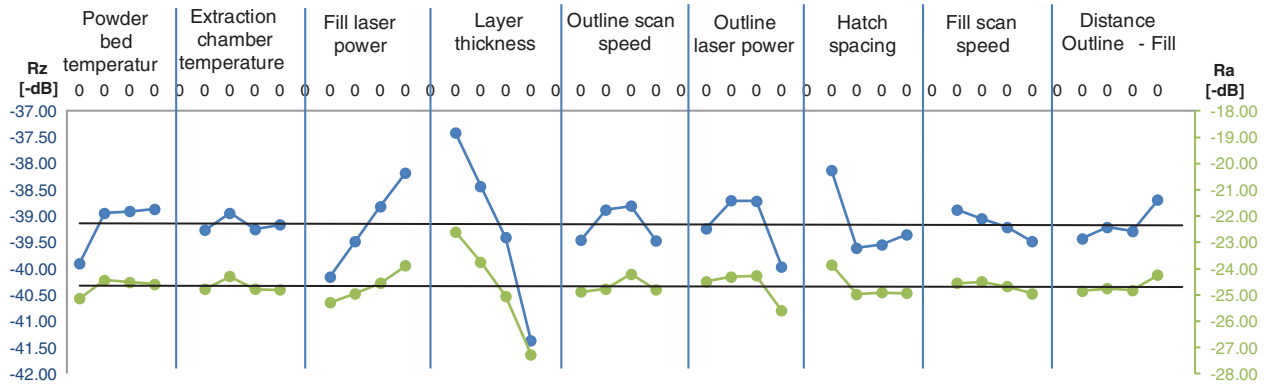


Fig. 5: ANOM chart for 30° downward facing surface.

orientation (except for the surface orientation parallel to the building platform, 0°) the ANOVA analysis confirms ANOM's results of having the layer thickness the most significant factor.

In the case of downward facing surfaces the laser power affects the surface roughness too. That may be due to the fact that with increasing laser power, the filleting effect increases at the same time and works against the stair stepping effect. In the case of upward facing surfaces the energy density does not affect the surface roughness.

The results, shown in figure 6, prove that part orientation is one of the most significant factors on surface roughness. On average the surface roughness depth of downward facing surfaces is about 32% better than the upward facing surfaces. This may be due to the filling effect observed on downward facing surfaces. It also shows that the surface becomes more inclined with decreasing degrees of orientations. Reasons can be found within the stair case effect which is pronounced more in dependence of the degree of orientation. Worst values can be found with an orientation of 15°.

3.1.3. Mechanical Properties

In the course of investigation 224 specimens for tensile test were built in the directions 0°, 15°, 30°, 45°, 60°, 75°, 90°. According to DIN EN ISO 527-1 and DIN EN ISO 10350-1 tensile test were performed to establish a correlation between process parameters, part orientation and part properties. To determine the significance of process parameters, the maximization problem is used. The main effects for tensile strength, young's module and elongation break are shown in figure 7. As you can see, all factor influences follow nearly the same trend.

Figure 7 shows that, with decreasing powder layer thickness, there is an improvement in all considered targets. This is due to the fact that the volume energy density E_V increases with declining powder layer thickness. Additionally all other parameters of the equation of the Energy density, compare Equation (3),

have a main influence on the mechanical properties of laser-sintered parts made of polypropylene. The influence of the extraction chamber temperature as well as the energy density of the outline scanning and distance between outline and fill exposure are, however, negligible and therefore pooled with in the ANOVA analysis. The significance of all factors is shown in table 4.

Regardless to the orientation of the built test specimen powder layer thickness and laser power of the fill exposure have the highest influence, rating up to 54%. Further significant factors are the laser power of the fill exposure and hatch spacing. The influences of both the temperatures and energy density of outline exposure are relatively low and are therefore excluded by associating them to the error.

Figure 8 shows the tensile strength as well as young's modulus and elongation break of laser-sintered parts in dependence of the orientation of the part. First of all, best mechanical properties can be reached with an orientation of 0°. Increasing the angle up to 75°, all mechanical properties deteriorate. This anisotropic effect could be observed with every test series. Compared to the surface orientation dependence the mechanical properties vary relatively low.

3.1.4. Curling

As shown in figure 1b, the dimensional deviation Δ_{curl} in building direction of the test body geometry was measured. All captured distances were used to perform the ANOM analysis. Here the minimization is used to identify main influences to the curl effect. Analog to the investigations of the mechanical properties 224 test body geometries were built in the directions 0°, 15°, 30°, 45°, 60°, 75°, 90°. A detailed view would again exceed the scope of this paper. For this reason just the most important results are presented. First of all, the temperatures of both powder bed and extraction chamber show a high significance for the curl effect. High temperature gradients between the actual melted layer geometry and ambient temperature foster curling. Thus the

F	0°		15°		30°		45°		60°		75°		90°		105°		120°		135°		150°		165°		180°		
	Siq	P [%]	Siq	P [%]	Siq	P [%]	Siq	P [%]	Siq	P [%]	Siq	P [%]	Siq	P [%]	Siq	P [%]	Siq	P [%]	Siq	P [%]	Siq	P [%]	Siq	P [%]	Siq	P [%]	
A	X			3,8	*	4,3	X	-	X	-	X	-	X	-		2,2		3,35		3,9	X	-	X	-			1,9
B		5,7		3,7	X		X			2,8	X			1,3	X			0,83		4,2	X	0,6	X	0,1			8,5
C	*	16,3	*	16,6	**	13,7		1,4		1,7	*	10,3	X		X		X		X		1,7	*	2,7				0,1
D		2,8	**	29,9	**	55,8	**	42,4	**	35,3	**	47,8	**	59,7	**	52,4	**	56,62	**	49,2	**	75,7	**	89,9	**	28,6	**
E	*	15,8		0,9		1,9	X		X			0,8		0,9	X		X				1,7		0,1		0,5		2,7
F		5,7	X		**	6,3	X			6,0		3,2		1,3		1,8		2,10		1,1		3,2	X				3,0
G	X			1,8	**	8,8	X		X		X			1,5		0,6		1,23		3,0	X			0,1	X		-
H	*	12,4	X			0,6	X			0,8	X			3,3		0,5	X		X		X		*	1,4	X		-
I	X			0,6		1,3	X		X			3,3	X			4,7		1,07		4,4		1,9		0,1	X		-

Tab. 3: ANOVA table for surface roughness.

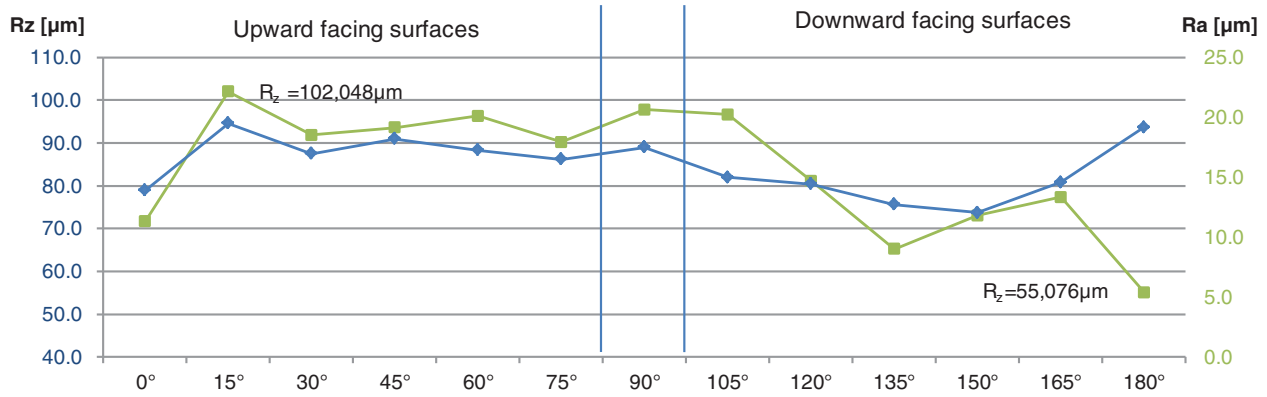


Fig. 6: Surface roughness for up- and downward facing surfaces.

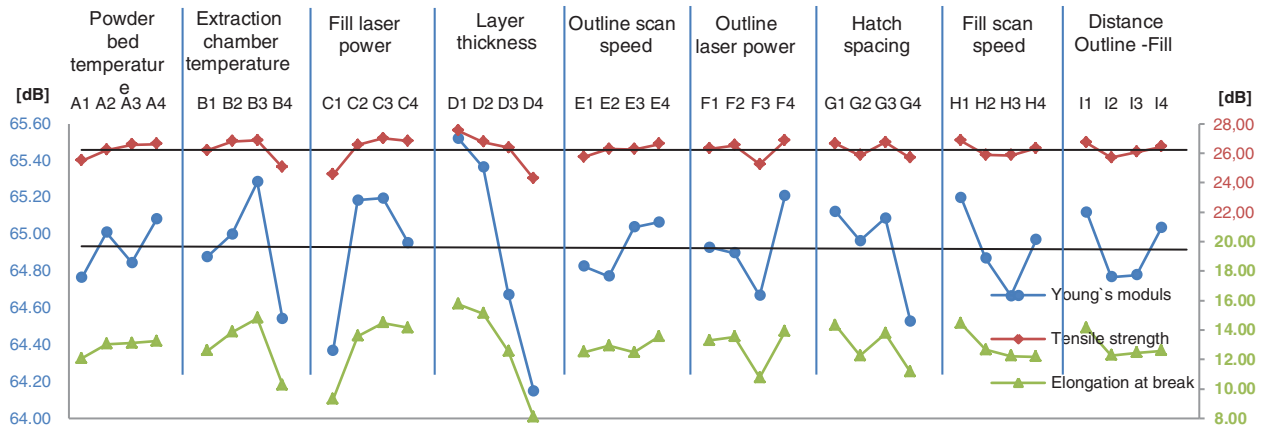


Fig. 7: ANOM chart for tensile strength, Young's module and Elongation at break.

volume energy density of fill exposure is decisive for minimizing the curl effect.

Fig. 9 shows the degree of curl in dependence of the length of the test body geometry. Here Point 1 shows the curling after $l = 0,5 \text{ mm}$, point 27 at a length of 135.5 mm . As expected the curl effect shows up most with an orientation of 0° . Here the largest surface is melt down in the first layer. With increasing angle the curl effect can be minimized. Minimum curl appears at an angle of 45° referred to the building platform. Inter alia the tests showed revealed a highly significant effect of the test body geometry. For an entirely statement about the curl mechanism, additional experiments are necessary.

Fig. 9 shows the degree of curl in dependence of the length of the test body geometry. Here Point 1 shows the curling after $l = 0,5 \text{ mm}$, point 27 at a length of 135.5 mm . As expected the curl effect shows up most with an orientation of 0° . Here the largest surface is melt down in the first layer. With increasing angle the curl effect can be minimized. Minimum curl appears at an angle of 45° referred to the building platform. Inter alia the tests showed revealed a highly significant effect of the test body geometry. For an entirely statement about the curl mechanism, additional experiments are necessary.

3.1.5. Discussion

The results of the Taguchi analysis were used to improve laser-sintered part properties such as dimensional and shape accuracy, surface roughness, mechanical properties and the reducing of the curl effect. In the course of investigations the significance of all process parameters were examined. In total powder layer thickness has the highest influence on all parameters studied. Reasons can be found within the stair stepping effect associated with the layer thickness. The lower the powder layer thickness the better the parts properties. Furthermore the density of fill exposure, represented by the laser power, turned out to be a significant factor. High energy densities of the fill exposure improve part properties such as surface roughness or mechanical properties, but lower the dimensional accuracy. Best properties could be found within the limits $E_{\min} = 0,15 \text{ J/mm}^3$, and $E_{\max} = 0,19 \text{ J/mm}^3$. The outline energy density is mostly responsible for the surface roughness. The surface finish improves with increasing energy density, but after a certain value the surface quality deteriorates. Recommended energy density for the outline exposure is in the range between $E_{\min} = 0,15 \text{ J/mm}$, and $E_{\max} = 0,19 \text{ J/mm}$. All in all does a

Orientation Factor	0°		15°		30°		45°		60°		75°		90°	
	Siq	P [%]	Siq	P [%]	Siq	P [%]	Siq	P [%]	Siq	P [%]n	Siq	P [%]	Siq	P [%]
a) tensile strength														
A Powder bed temperature	*	11,1	**	12,7				0,2	X	-		5,3		5,0
B Extraction chamber temperature	X	-		3,7	*	7,6	*	9,0	X	-		8,4		5,0
C Fill laser power		6,8	**	12,7	*	13,6	**	22,7		4,4		8,2	*	18,5
D Layer thickness	**	31,9	**	32,2	**	40,7	**	25,9	*	23,7	*	22,5	**	28,6
E Outline scan speed		1,4	X	-	X	-	X	-	X	0,3	X	-	X	-
F Outline laser power	X	-	**	12,3		2,7	X	-	X	-	X	0,3		0,2
G Hatch spacing		1,5		2,6		5,5	X	-		0,8	X	-	X	-
H Fill scan speed		0,2		1,9		2,7	X	-		3,9		0,2	X	-
I Distance Outline - Fill	X	-	X	-		0,9	X	-		5,1		1,6		1,0
b) Young's module														
A Powder bed temperature		3,5		0,8		0,2	X	-	X	-		8,4		4,2
B Extraction chamber temperature		2,9		4,2		7,5		4,6		0,3	*	15,4	*	8,4
C Fill laser power	**	21,8	*	18,4	*	17,0	*	16,3		3,5		6,8	**	16,8
D Layer thickness	**	34,3	**	30,1	**	27,2	**	32,7	**	28,6	*	32,4	**	30,0
E Outline scan speed	X	-	X	-	X	-	X	-		1,9		0,3	X	-
F Outline laser power		1,9		5,3		3,7		0,2	X	-		3,7	X	-
G Hatch spacing	X	-	X	-		0,6	X	-		7,1		6,1	X	-
H Fill scan speed		2,1		0,6	X	-		2,3		8,0		3,5		6,2
I Distance Outline - Fill		0,2	X	-	X	-	X	-		2,5		1,0		0,9
c) Elongation at break														
A Powder bed temperature	X	-	X	-	X	-	X	-	X	-		1,4		1,6
B Extraction chamber temperature		8,8	*	9,1	*	10,6		2,8		0,5		8,8	*	5,5
C Fill laser power	**	21,4	*	15,8	**	17,3	*	10,4		1,7		1,9	**	12,2
D Layer thickness	**	21,3	**	26,8	**	38,2	**	46,5	**	45,8	**	54,7	**	52,7
E Outline scan speed	X	-	X	-	X	-	X	-		4,4		0,1	X	-
F Outline laser power		0,4		4,0		4,6		0,8	X	-		0,9	X	-
G Hatch spacing		5,8		5,3		4,8		5,7	*	13,0	*	13,6		1,1
H Fill scan speed		0,7		0,8		1,5		3,0		6,2		0,0		5,2
I Distance Outline - Fill	X	-	X	-		0,3		0,6		0,5		2,0		1,0

Tab. 4: ANOVA table for tensile strength, Young's module and Elongation at break.

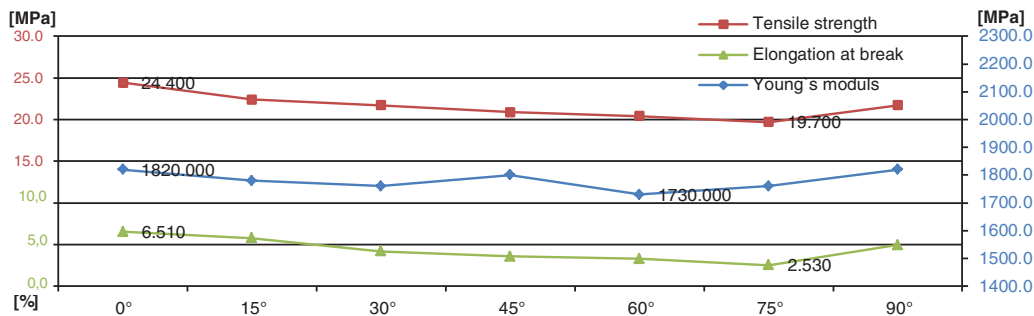


Fig. 8: Mechanical properties in dependence of the part orientation.

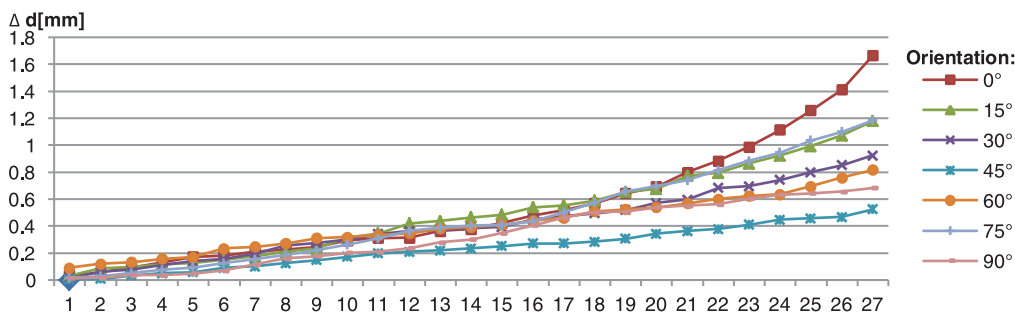


Fig. 9: Curling in Dependence of the part orientation.

higher temperatures provide a greater energy input into the powder bed and positively influence mechanical part properties up to the limit of $t_{\max} = 141^{\circ}\text{C}$. It is opposed by a decrease of the dimensional accuracy and surface quality. The powder bed temperature should be set between $t_{\min} = 139^{\circ}\text{C}$ to $t_{\max} = 140^{\circ}\text{C}$ and the temperature of the extraction chamber should be adjusted to 100°C . The same applies to the extraction chamber temperature. Summarized the optimized parameter settings found improve all investigated part properties.

3.2. Part Orientation

Based on the findings of the process optimization, a multi-objective approach for the part orientation is used. Therefore the identified effects for part quality and process efficiency are taken into account. Adapted from this input parameters, DANJOU and KÖHLERS genetic optimization algorithm (see figure 11) is used to determine the optimal orientation. Starting with a preparation step, the part geometry is imported as STL file, then the convex hull is constructed and extreme dimensions are determined. Subsequent the genetic algorithm is initialized. Afterwards, the part is rotated in different angles and for each orientation the part is sliced and evaluated for the identified effects like volume, cusp height, build time, max. exposure area, etc. The combination of these effects result in a fitness analysis for each examined orientation. As long as this

function does not reach convergence a recombination, mutation and selection of a new population leads to a new calculation. When the fitness analysis reaches convergence, the suggested orientations are exported as STL files in the new orientation [4–6].

Hence DANJOU and KÖHLERS approach deliver suitable results some adjustments have to be done for the implementation of the experimental results. This is exemplarily shown for the influencing factor surface roughness. This influencing variable can be identified as key impact for the part orientation hence the so called “stair case effect” that occurs because of the characteristic layer by layer manufacturing of the parts always influences the surface quality of curved and inclined surfaces. Figure 11 shows in an exaggerated way how this effect depends on the pitch of the inclined up- and down-facing surfaces. The detail view (see figure 11c) reveals another problem. Faces that were created with a different pitch may be combined due to the slicing algorithm. However, vertically positioned faces are the best possible orientation and therefore it can be assumed in the first way, that the orientation that consists of the most vertically positioned faces should be favoured.

When only these geometric influences are taken into account for the optimization of the orientation, two different approaches may be used in order to quantify the error that is caused by the stair casing effect. The first option is to measure the exact volume deviation between the faced (STL) and the layer model. Therefore the volume of the layer model has to

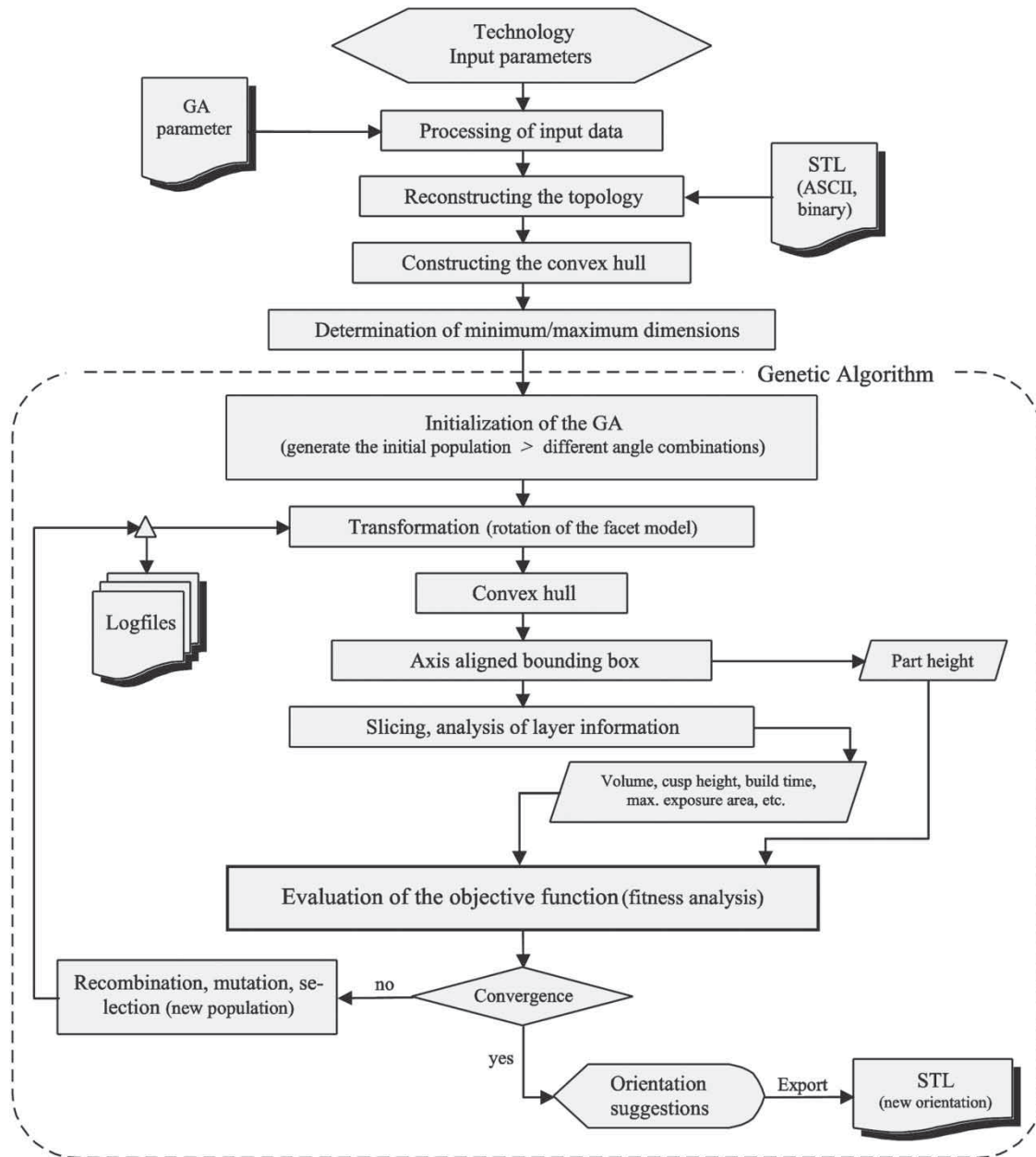


Fig. 10: Optimization algorithm (based on [4]).

be calculated for each orientation. This can be reached by direct slicing of the CAD geometry or layer by layer calculation of the volume by using the created contours and the layer thickness (cf. figure 12a). However, both ways are time consuming and therefore influencing the optimization performance. Regarding this the so called cusp height approach is used. The cusp height is a variable that describes the maximal deviation in a virtual error triangle (cf. Figure 12b). This method delivers comparable fast and good results for the qualification of volume error [4].

Figure 13 shows how the cusp height of the sliced geometry is influenced by the pitch of the face and

the layer thickness. Because only the pitch of the in- and declined faces is considered the absolute value of the cusp height is equal for mirrored surfaces like 45° (upward faced) and 135° (downward faced). Compared with the experimental results (dashed curve) the influence of the layer thickness in combination with the pitch of the surface can be proven. Nevertheless, some deviations of the experimental results have to be considered. As described the geometry based analysis of the surface quality delivers the same values for comparable angles of the in- and declined faces. Yet, the experimental results have shown that a significant divergence exists for these causes.

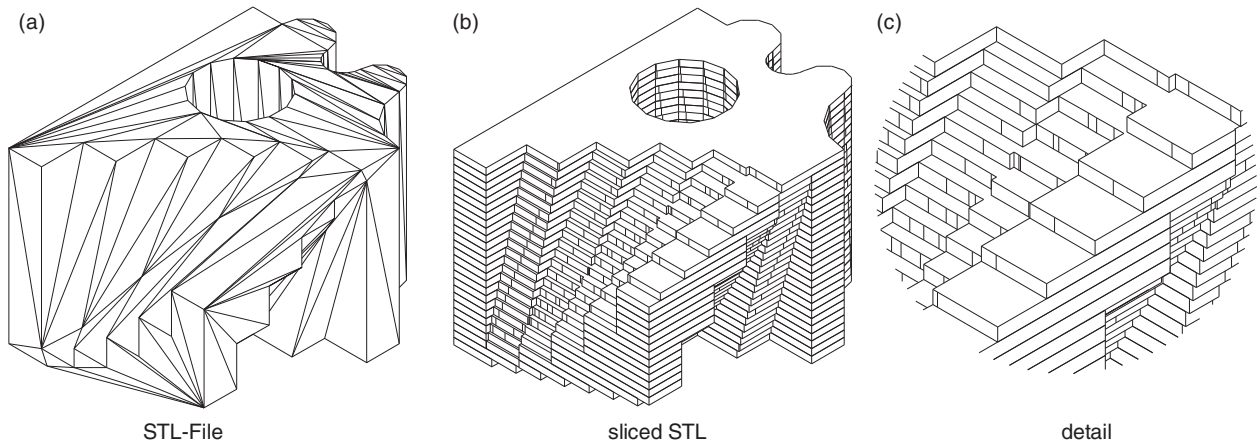


Fig. 11: Stair case effect.

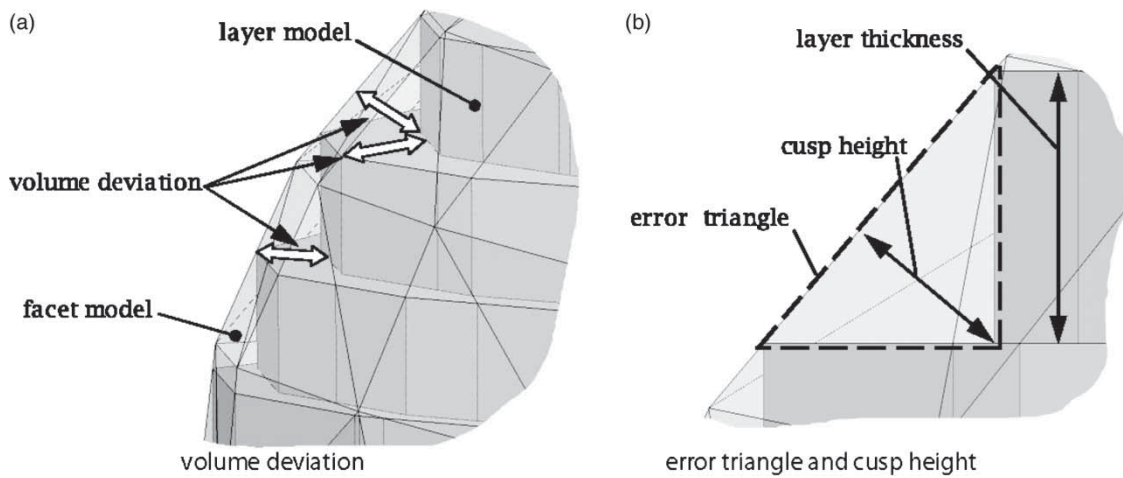


Fig. 12: Geometry-based qualifying the staircase effect error [4].

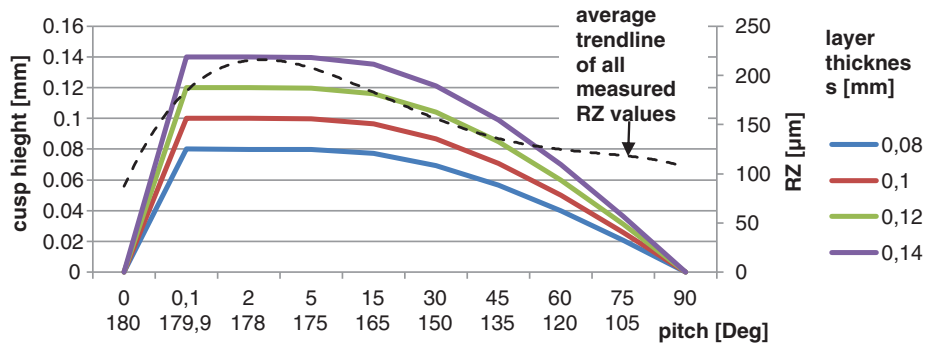


Fig. 13: Inclined faces and their cusp height for different layer thicknesses.

As pointed out in paragraph 3.1.2 the downward faced surfaces have an up to 30% better surface quality than the upward faced ones. This has to be considered for the optimization process. Regarding this result, a correction factor is used in order to favor face orientations with a higher amount of downward faced surfaces. Since the experimental results have proven

that the quality trend is comparable with the results of the geometrical investigations (cf. figure 13) the cusp height approach delivers comprehensive results for the optimization of the orientation and can therefore be used. Beside the factor regarding the face orientation the assumption that vertically positioned faces deliver the best performance can be proven as

wrong. Even if this assumption is correct when only the geometry is regarded the manufacturing process leads to rough vertical walls (chapter 3.1.2). Therefore slightly cocked faces should be preferred for the optimization.

4. CONCLUSION

The results of all experiments have proven that the part orientation influences the part quality and the process efficiency. Moreover, it was shown that a conjunction between experimental results and software strategies for the optimization of the part orientation is feasible. Yet, these experiments also indicate problems that occur when only the part geometry is considered for the optimization of the part orientation. Therefore the execution of comprehensive experiments is necessary when software based optimization results should deliver effective solutions. In this regard more experiments for different AM processes, materials and parameters have to be realized in order to create widespread solutions.

REFERENCES

- [1] Byun, H. S.; Lee, K. H.: Determination of Optimal Part Orientation in Layered Manufacturing Using a Genetic Algorithm, *Int. J. Prod. Res.*, 43(13), 2005, 2709-2724. <http://dx.doi.org/10.1080/00207540500031857>
- [2] Caulfield, B.; McHugh, P.E.; Lohfeld, S.: Dependence of mechanical properties of polyamide components on build parameters in the SLS process, In: *Journal of Materials Processing Technology*, Bd. 182 (2007) Nr. 1-3, S. 477-488.
- [3] Cheng, W.; Fuh, J.; Nee, A.; Wong, Y.; Loh, H.; Miyazawa, T.: Multi-Objective Optimization of Part-Building Orientation in Stereolithography, *Rapid Prototyping Journal*, 1(4), 1995, 12-23.
- [4] Danjou, S., Köhler P.: Determination of Optimal Build Direction for Different Rapid Prototyping Applications, *Proceedings of the 14th European Forum on Rapid Prototyping*, 2009.
- [5] Danjou, S., Köhler P.: Multi-Objective Optimization of Part Orientation for Non-Convex Parts in Rapid Technology Applications, *Proceedings of the 10th national Conference on Rapid Design, Prototyping & Manufacture*, 2009, 81-90.
- [6] Danjou, S.: *Mehrzieloptimierung der Bauteilorientierung für Anwendungen der Rapid-Technologie*, Cuvillier, Göttingen, 2010.
- [7] Gebhardt, A.: *Generative Fertigungsverfahren. Rapid Prototyping - Rapid Tooling - Rapid Manufacturing*, Carl Hanser Verlag, München, 2007.
- [8] Gornet, T.: *Materials and Process Control for Rapid Manufacture*. In: *Rapid Manufacturing - An Industrial Revolution For The Digital Age*, 1. Auflage, John Wiley & Sons, West Sussex, 2006.
- [9] Masood, S. H.; Rattanawong, W.: Generic Part Orientation System Based on Volumetric Error in Rapid Prototyping, *International Journal of Advanced Manufacturing Technology*, 19(3), 2002, 209-216.
- [10] Pham, D. T.; Dimov, D. T.; Gault, R. S.: Part Orientation in Stereolithography, *International Journal of Advanced Manufacturing Technology*, 15(9), 1995, 674-682. <http://dx.doi.org/10.1007/s001700050118>
- [11] Sauer, A.: *Optimierung der Bauteileigenschaften beim Selektiven Lasersintern von Thermoplasten*; Dissertation, Universität Duisburg-Essen, 2005.
- [12] The Association of German Engineers 2009 VDI Guideline 3404: *Additive fabrication - Rapid technologies (rapid prototyping) Fundamentals, terms and definitions, quality parameters, supply agreements*, Beuth Verlag, Berlin
- [13] Tyagi, S. K.; Ghorpade, A.; Karunakaran, K. P.; Tiwari, M. K.: Optimal Part Orientation in Layered Manufacturing Using Evolutionary Stickers-Based DNA Algorithm, *Virtual and Physical Prototyping*, 2(1), 2007, 3-19. <http://dx.doi.org/10.1080/17452750701330968>
- [14] Wohlers, T.: *Wohlers Report 2011: Additive Manufacturing and 3D-Printing, State of the Industry, Annual Worldwide Prozess Report*, Wohlers Associates, Colorado, USA, 2011.
- [15] Yang, Z. Y.; Chen, Y. H.; Sze, W. S.: Determining Build Orientation for Layer-Based Machining, *International Journal of Advanced Manufacturing Technology*, 18 (5), 2001, 313-322. <http://dx.doi.org/10.1007/s001700170055>
- [16] Xu, F.; Loh, H. T.; Wong, Y. S.: Considerations and Selection of Optimal Orientation for Different Rapid Prototyping Systems, *Rapid Prototyping Journal*, 5(2), 1999, 54-60. <http://dx.doi.org/10.1108/13552549910267344>